Charge-Transfer Complexes of 4-Phenyl-1,2,3,5-dithiadiazolyl and 4-Phenyl-1,2,3,5-diselenadiazolyl with Iodine. Preparation and Solid-State Characterization of $[PhCN_2E_2]_3[I_3]$ (E = S, Se) and $[PhCN_2S_2][I_3]$

C. D. Bryan,[1a] A. W. Cordes,*[,1a] R. C. Haddon,*[,1b] R. G. Hicks,[1c] R. T. Oakley,*[,1c] T. T. M. Palstra,[1b] A. S. Perel,[1b] and S. R. Scott[1a]

Department of Chemistry and Biochemistry, University of Arkansas, Fayetteville, Arkansas 72701; AT&T Bell Laboratories, 600 Mountain Ave., Murray Hill, New Jersey 07974; Guelph-Waterloo Centre for Graduate Work in Chemistry, Guelph Campus, Department of Chemistry and Biochemistry, University of Guelph, Guelph, Ontario, N1G 2W1, Canada

Received December 16, 1993. Revised Manuscript Received February 4, 1994[⊗]

The 1:1 reaction of the heterocyclic radicals $[PhCN_2E_2]^\bullet$ (E = S, Se) and iodine affords the mixed valence salts $[PhCN_2E_2]_3[I_3]$, while reaction of $PhCN_2S_2$ with an excess of iodine affords the simple salt $[PhCN_2S_2][I_3]$; the solid-state structures of these complexes have been determined by X-ray crystallography. Crystals of both of the mixed valence compounds belong to the triclinic space group $P\bar{1}$; for E = S, α = 10.278(4), b = 11.508(2), c = 13.333(4) Å, α = 114.97(2), β = 99.21 (3), γ = 92.65(2)°, FW = 308.15, Z = 6; for E = Se, a = 10.368(6), b = 10.818(8), c = 13.421(8) Å, α = 80.64(5), β = 81.20(5), γ = 75.18(6)°, FW = 401.95, Z = 6. Crystals of the simple salt belong to the monoclinic space group $P2_1/a$; a = 7.366(4), b = 11.734(1), c = 15.166(2) Å, β = 95.92(3)°, FW = 1303.99(7), Z = 4. In each of the mixed valence compounds the molecular (asymmetric) unit consists of a trimeric $[PhCN_2E_2]_3^+$ cation and an associated triiodide anion. Within the cations the mean interannular E–E contacts are 3.181/3.377 Å (E = S/Se). The packing patterns of the two compounds show important differences. For E = S the crystal structure does not exhibit stacking of the trimeric molecular building blocks, but for E = Se the trimer units form dovetailed stacks in which consecutive layers are oriented in a trans-antipodal fashion. This arrangement introduces close interannular contacts between the blocks along the stack, as well as close lateral contacts. The asymmetric unit of $[PhCN_2S_2][I_3]$ consists of a single $PhCN_2S_2^+$ cation and an associated triiodide anion; there are no unusual stacking features. The magnetic and conductivity properties of $[PhCN_2Se_2]_3[I_3]$ are reported, and the results discussed in the light of extended Hückel band structure calculations.

Introduction

The chemical and physical properties of heterocyclic thiazyl and selenazyl radicals have been investigated by several research groups.[2] Much of our work in this area has focused on derivatives of 1,2,3,5-dithiadiazolyl and 1,2,3,5-diselenadiazolyl 1(E = S, Se),[3] our intent being to design neutral π-radicals that will serve as building blocks for molecular conductors.[4] To this end we have prepared

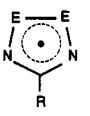

1

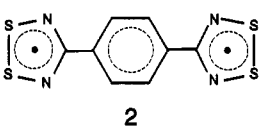

2

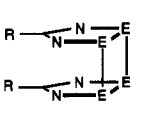

3

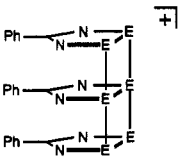

4

a wide range of mono-, di-, and trifunctional radicals (and their dimers), determined their solid-state structures and measured their transport properties.[5,6]

While considerable advances have been made in the synthesis and characterization of the neutral materials, the use of the radicals as donors for the generation of

⊗ Abstract published in *Advance ACS Abstracts*, March 15, 1994.

(1) (a) University of Arkansas. (b) AT&T Bell Laboratories. (c) University of Guelph.

(2) For example, see: (a) Dormann, E.; Nowak, M. J.; Williams, K. A.; Angus, R. O., Jr.; Wudl, F. *J. Am. Chem. Soc.* **1987**, *109*, 2594. (b) Wolmershäuser, G.; Wortmann, G.; Schnauber, M. *J. Chem. Res., Synop.* **1988**, 358. (c) Wolmershäuser, G.; Kraft, G.; *Chem. Ber.* **1990**, *123*, 881. (d) Awere, E. G.; Burford, N.; Haddon, R. C.; Parsons, S.; Passmore, J., Waszczak, J. V.; White, P. S. *Inorg. Chem.* **1990**, *29*, 4821. (e) Preston, K.; Sutcliffe, L. H. *Magn. Reson. Chem.* **1990**, *28*, 189. (f) Banister, A. J.; Rawson, J. M. In *The Chemistry of Inorganic Ring Systems*; Elsevier: Amsterdam, Ed. R. Steudel, 1992, p. 323.

(3) Cordes, A. W.; Haddon, R. C.; Oakley, R. T. In *The Chemistry of Inorganic Ring Systems*; Steudel, R., Elsevier: Amsterdam, Ed.; 1992.; p 295.

(4) (a) Haddon, R. C. *Nature (London)* **1975**, *256*, 394. (b) Haddon, R. C. *Aust. J. Chem.* **1975**, *28*, 2343.

(5) (a) Cordes, A. W.; Haddon, R. C.; Hicks, R. G.; Oakley, R. T.; Palstra, T. T. M. *Inorg. Chem.* **1992**, *31*, 1802. (b) Cordes, A. W.; Chamchoumis, C. M.; Hicks, R. G.; Oakley, R. T.; Young, K. M.; Haddon, R. C. *Can. J. Chem.* **1992**, *70*, 919.

0897-4756/94/2806-0508$04.50/0

charge transfer (CT) salts has been largely unexplored. There was an early suggestion that the phenyl derivative (R = Ph, E = S) formed a thermally unstable iodide salt, but no experimental details were provided.[7] The layered salt $[PhCN_2S_2]^+[S_3N_3]^-$ and the mixed dimer/cation salt $[CF_3CN_2S_2]_3[Cl]$ have also been described.[8,9] Recently, however, we reported the preparation and structural characterization of two highly conductive mixed valence salts, one based on the prototypal radical 1 (E = S, R = H), i.e., $[1]_6[I]_{1.1}$,[10] and the other on the bifunctional 1,4-phenylene derivative 2, i.e., [2][I].[11] In both compounds the molecular building blocks form uniformly spaced stacks (at ambient temperatures), with the iodines aligned in one-dimensional arrays exhibiting disorder along the stacking direction. In the case of [2][I] the conductivity is metallic at room temperature, but below 190 K a charge density wave (CDW) driven instability sets in and the conductivity drops sharply. Analysis of the CDW wave vector indicates a degree of charge transfer corresponding to the formulation $[2]^{+1/2}[I]^{-1/2}$.

As a further exploration of the structural consequences of partial oxidation of both dithia- and diselenadiazolyls, we have investigated the reaction of 1 (R = Ph; E = S, Se) with iodine. Two classes of iodide salts have been prepared and structurally characterized: (i) the mixed valence salts of nominal composition [1][I] and (ii) a simple triiodide salt of the dithiadiazolium cation, i.e., $[1][I_3]$. In contrast to the neutral radicals, which associate in the solid state as dimers, e.g., 3, and to the previously reported mixed valence dithiadiazolyl/iodine complexes noted above, we have found that the 1:1 CT salts of the phenyl derivatives are based on the novel triple-decker cation $[PhCN_2E_2]_3^+$, 4 (E = S, Se), associated with a triiodide anion. Herein we describe the synthesis, crystal structures, and transport properties of these materials, and discuss the results in light of extended Hückel band structure calculations.

Results and Discussion

Synthesis. The reaction of 1 (R = Ph, E = S) with iodine can be performed either in solution or in the gas phase. When carried out in solution, equivalent quantities (1:1) of iodine and radical are dissolved in refluxing acetonitrile. Upon slow cooling of the dark red solution very fine, almost hairlike, blue needles of composition $PhCN_2S_2I$ are produced. The compound can also be prepared, as suggested by Banister,[7] by a metathesis reaction between $[PhCN_2S_2][Cl]$ and KI. Larger needles, with the same composition and infrared spectrum, can be grown by very slow sublimation of the two reagents in a sealed, evacuated tube (see Experimental Section). While material suitable for bulk analysis was obtained in several days, crystals suitable for X-ray work required a long (5-week) sublimation period. The reaction involving (1 (R = Ph, E = Se) and iodine is best performed by the gas-phase route, although it too can be made in microcrystalline form by metathesis of $[PhCN_2Se_2][PF_6]$ with n-Bu_4NI in acetonitrile. Crystals of the selenium-containing product obtained by cosublimation with iodine are nominally larger than those of the corresponding sulfur compound, but prolonged sublimation times are again critical in order to obtain crystals suitable for X-ray work. As confirmed below, the structural unit in both these 1:1 compounds (E = S and Se) is $[PhCN_2E_2]_3[I_3]$.

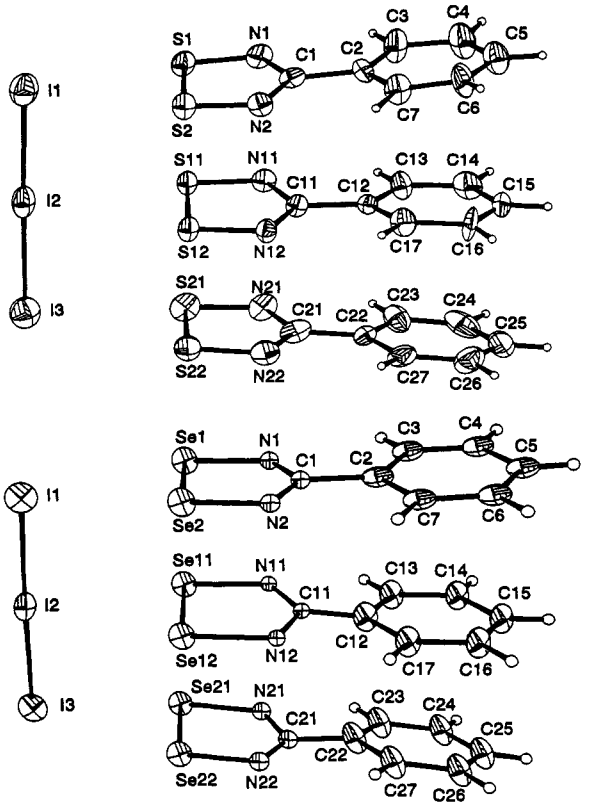

Figure 1. ORTEP drawings (30% ellipsoids) of $[PhCN_2E_2]_3[I_3]$, E = S (above) and Se (below). The interannular E–E bonds are omitted for clarity.

In addition to the 1:1 compounds described above, we have been able to isolate a salt of composition $[PhCN_2S_2][I_3]$ by cosublimation of iodine and radical in a molar ratio of greater than 3:1. Structural analysis on this material (below) shows it to be a simple triiodide salt $[PhCN_2S_2][I_3]$.

Crystal Structures. Crystals of both $[PhCN_2E_2]_3[I_3]$ (E = S, Se), obtained as described above, belong to the triclinic space group $P\bar{1}$. ORTEP drawings of the asymmetric units are provided in Figure 1, and atomic (non-hydrogen) coordinates are listed in Tables 1 and 2. A summary of pertinent bond lengths and angles within the asymmetric units is shown in Table 3, and interannular contacts are listed in Table 4.

(6) (a) Cordes, A. W.; Haddon, R. C.; Oakley, R. T.; Schneemeyer, L. F.; Waszczak, J. V.; Young, K. M.; Zimmerman, N. M. *J. Am. Chem. Soc.* **1991**, *113*, 582. (b) Andrews, M. P.; Cordes, A. W.; Douglass, D. C.; Fleming, R. M.; Glarum, S. H.; Haddon, R. C.; Marsh, P.; Oakley, R. T.; Palstra, T. T. M.; Schneemeyer, L. F.; Trucks, G. W.; Tycko, R.; Waszczak, J. V.; Young, K. M.; Zimmerman, N. M. *J. Am. Chem. Soc.* **1991**, *113*, 3559. (c) Cordes, A. W.; Haddon, R C.; Hicks, R. G.; Oakley, R. T.; Palstra, T. T. M.; Schneemeyer, L. F.; J. V. Waszczak, L. F. *J. Am. Chem. Soc.* **1992**, *114*, 1729. (d) Cordes, A. W.; Haddon, R. C.; Hicks, R. G.; Kennepohl, D. K.; Oakley, R. T.; Palstra, T. T. M.; Schneemeyer, L. F.; Scott, S. R.; Waszczak, J. V. *Chem. Mater.* **1993**, *5*, 820. (e) Cordes, A. W.; Haddon, R. C.; Hicks, R. G.; Oakley, R. T.; Palstra, T. T. M.; Schneemeyer, L. F.; Waszczak, J. V. *J. Am. Chem. Soc.* **1992**, *114*, 5000.

(7) Banister, A. J.; Smith, N. R. M.; Hey, R. G. *J. Chem. Soc., Perkin Trans. 1*, **1983**, 1181.

(8) Banister, A. J.; Hansford, M. I.; Hauptman, Z. V.; Luke, A. W.; Wait, S. T.; Clegg, W.; Jorgensen, K. A. *J. Chem. Soc., Dalton Trans.* **1990**, 2793.

(9) Höfs, H. U.; Mews, R.; Clegg, W.; Noltemeyer, M.; Schmidt, M.; Sheldrick, G. M. *Chem. Ber.* **1985**, *118*, 3781.

(10) Bryan, C. D.; Cordes, A. W.; Haddon, R. C.; Hicks, R. G.; Kennepohl, D. K.; MacKinnon, C. D.; Oakley, R. T.; Palstra, T. T. M.; Perel, A. S.; Scott, S. R.; Schneemeyer, L. F.; Waszczak, J. V. *J. Am. Chem. Soc.* **1994**, *116*, 1205.

(11) Bryan, C. D.; Cordes, A. W.; Fleming, R. M.; George, N. A.; Glarum, S. H.; Haddon, R. C.; Oakley, R. T.; Palstra, T. T. M.; Perel, A. S.; Schneemeyer, L. F.; Waszczak, J. V. *Nature* **1993**, *365*, 821.

Table 1. Non-Hydrogen Atomic Parameters x, y, z, and B_{eq} for 4 (E = S). ESDs Refer to the Last Digit Printed

	x	y	z	B_{eq}[a]
I1	0.19985(10)	0.72906(11)	0.75332(9)	5.84(7)
I2	0.16361(9)	0.44320(11)	0.64394(8)	4.75(6)
I3	0.13084(10)	0.16338(11)	0.54076(9)	5.93(7)
S1	0.1611(3)	0.7405(3)	1.0079(3)	3.58(20)
S2	0.3594(3)	0.7318(3)	1.0040(3)	3.56(19)
S11	0.1234(3)	0.4277(3)	0.8965(3)	3.12(19)
S12	0.3253(3)	0.4275(3)	0.8945(3)	2.87(18)
S21	0.0855(3)	0.1267(4)	0.7810(3)	4.27(22)
S22	0.2838(3)	0.1161(4)	0.7738(3)	4.50(23)
N1	0.1759(10)	0.7513(10)	1.1319(9)	3.6(7)
N2	0.4015(9)	0.7411(10)	1.1270(9)	3.5(6)
N11	0.1377(10)	0.4300(10)	1.0202(8)	3.2(6)
N12	0.3648(9)	0.4254(9)	1.0147(8)	3.0(6)
N21	0.1017(11)	0.1196(11)	0.9004(10)	4.4(7)
N22	0.3238(10)	0.1071(10)	0.8928(10)	4.1(7)
C1	0.3003(12)	0.7530(11)	1.1835(11)	3.0(8)
C2	0.3252(13)	0.7707(11)	1.3020(10)	3.1(7)
C3	0.2258(13)	0.7896(14)	1.3630(13)	4.4(9)
C4	0.2559(18)	0.8082(15)	1.4719(13)	5.7(11)
C5	0.3776(15)	0.7998(14)	1.5211(12)	5.0(10)
C6	0.4755(14)	0.7785(17)	1.4602(14)	6.1(12)
C7	0.4524(13)	0.7654(16)	1.3508(13)	5.3(11)
C11	0.2628(12)	0.4273(11)	1.0668(11)	2.8(7)
C12	0.2888(13)	0.4293(11)	1.1791(10)	2.8(7)
C13	0.1889(14)	0.4496(13)	1.2426(13)	4.3(8)
C14	0.2117(15)	0.4447(15)	1.3457(12)	4.8(10)
C15	0.3315(16)	0.4288(13)	1.3889(11)	4.2(8)
C16	0.4346(13)	0.4111(14)	1.3294(13)	4.8(10)
C17	0.4119(13)	0.4114(13)	1.2254(12)	3.7(8)
C21	0.2221(14)	0.1108(12)	0.9455(13)	3.8(9)
C22	0.2467(13)	0.0975(11)	1.0493(11)	3.3(7)
C23	0.1486(13)	0.1100(13)	1.1119(13)	4.4(9)
C24	0.1711(15)	0.0992(15)	1.2134(14)	5.5(11)
C25	0.2937(19)	0.0725(14)	1.2533(13)	5.3(10)
C26	0.3887(17)	0.0607(14)	1.1887(16)	5.8(10)
C27	0.3684(15)	0.0751(13)	1.0914(13)	4.5(8)

[a] B_{eq} is the mean of the principal axes of the thermal ellipsoid.

Table 2. Non-Hydrogen Atomic Parameters x, y, z, and B_{eq} for 4 (E = Se). ESDs Refer to the Last Digit Printed

	x	y	z	B_{eq}[a]
I1	0.7337(7)	0.5321(6)	0.8375(5)	4.8(4)
I2	0.4583(8)	0.6856(6)	0.8445(5)	3.9(3)
I3	0.1809(7)	0.8434(6)	0.8446(5)	4.8(4)
Se1	0.8376(9)	0.6542(8)	0.5829(7)	3.15(15)
Se2	0.7816(9)	0.4614(8)	0.5854(7)	3.15(15)
Se11	0.5245(9)	0.8291(8)	0.5869(7)	3.15(15)
Se12	0.4568(9)	0.6405(8)	0.5881(7)	3.15(15)
Se21	0.1933(9)	1.0070(8)	0.5959(7)	3.15(15)
Se22	0.1439(9)	0.8119(8)	0.5949(7)	3.15(15)
N1	0.857(6)	0.677(4)	0.449(4)	2.0(8)
N2	0.800(5)	0.476(4)	0.455(4)	2.0(8)
N11	0.547(5)	0.855(4)	0.447(4)	1.7(8)
N12	0.477(5)	0.664(4)	0.441(4)	1.7(8)
N21	0.195(5)	1.043(4)	0.455(4)	2.4(8)
N22	0.149(5)	0.836(4)	0.464(4)	2.4(8)
C1	0.839(7)	0.580(5)	0.406(3)	2.0(8)
C2	0.861(5)	0.608(5)	0.289(3)	3.4(18)
C3	0.909(5)	0.712(4)	0.234(4)	3.4(18)
C4	0.935(5)	0.720(4)	0.129(4)	3.4(18)
C5	0.914(5)	0.626(5)	0.078(3)	3.4(18)
C6	0.867(5)	0.522(4)	0.133(4)	3.4(18)
C7	0.840(5)	0.513(4)	0.239(4)	3.4(18)
C11	0.517(6)	0.770(5)	0.398(2)	1.7(8)
C12	0.522(6)	0.778(6)	0.297(3)	5.0(23)
C13	0.553(6)	0.892(5)	0.247(4)	5.0(23)
C14	0.567(6)	0.914(5)	0.141(4)	5.0(23)
C15	0.550(6)	0.823(6)	0.085(3)	5.0(23)
C16	0.519(6)	0.709(5)	0.135(4)	5.0(23)
C17	0.505(6)	0.686(5)	0.241(4)	5.0(23)
C21	0.171(7)	0.948(5)	0.414(2)	2.4(8)
C22	0.194(6)	0.965(6)	0.303(3)	4.6(21)
C23	0.200(6)	1.087(5)	0.252(4)	4.6(21)
C24	0.198(6)	1.111(4)	0.147(4)	4.6(21)
C25	0.191(6)	1.014(5)	0.093(3)	4.6(21)
C26	0.185(6)	0.892(5)	0.144(4)	4.6(21)
C27	0.187(6)	0.867(4)	0.249(4)	4.6(21)

[a] B_{eq} is the mean of the principal axes of the thermal ellipsoid.

Table 3. Summary of Intramolecular Distances (angstroms) and Angles (degrees) in 4 (E = S, Se)[a]

	E = S		E = Se	
	outer	inner	outer	inner
E–E	2.059(9)	2.080(4)	2.298(19)	2.318(14)
E–N	1.60(4)	1.61(2)	1.77(14)	1.89(10)
N–C	1.34(4)	1.34(2)	1.34[b]	1.34[b]
I1–I2	2.958(2)		2.909(10)	
I2–I3	2.896(2)		2.945(10)	
I–I–I	178.92(5)		178.2(3)	
E1–E11	3.239(5)		3.310(12)	
E2–E12	3.150(5)		3.428(12)	
E11–E21	3.114(5)		3.476(12)	
E12–E22	3.222(5)		3.295(12)	

[a] Numbers in parentheses are ESDs for single-valued parameters. For averaged distances the number is the greater of the range and ESD. The terms "outer" and "inner" refer to the three rings (two outer and one inner) within the trimeric $[PhCN_2E_2]_3^+$ cation. [b] The C–N distances were set as part of a rigid group.

The $[PhCN_2S_2]^+$ cation forms simple salts with a wide range of anions, several of which (with the anions Cl^-,[12] AsF_6^- [13]) have been characterized by X-ray crystallography; the crystal structures show few unusual features. The structure of the $[PhCN_2Se_2]^+$ cation, in its PF_6^- salt, has also been determined[14] and it too consists of discrete cations and anions. The $[PhCN_2E_2]_3^+$ trimer reported here is thus a hitherto unobserved molecular unit. Although one other radical dimer/cation structure has been reported, the dimer and cation units were quite separate.[9] In the present case the coplanar arrangement of three heterocycles is presumably favored by the proximity of the triiodide anion, to which the three rings are linked by a series of short E- - -I contacts (mean d(E- - -I) is 3.502/3.543 Å for E = S/Se). This "head-on" orientation of ion-pairing to a halide is not uncommon. It is observed in the CT salt [2][I] (although the iodines are disordered)[11] and also in simple dithiadiazolium salts, such as in $[PhCN_2S_2]$-[Cl], where the chloride ion lies in the molecular plane and aligns itself (approximately) equidistant from the two sulfur atoms. In both of the present structures the triiodide unit is essentially linear and symmetrical.

Within the three heterocyclic rings of 4 the E–N and E–E distances are longer than those found in simple $[PhCN_2E_2]^+$ cations, e.g., in the structures of $[PhCN_2S_2]$-$[AsF_6]$[13] and $[PhCN_2Se_2][PF_6]$,[14] but shorter than in the radical dimers 3 (R = Ph, E = S[15] and Se[14]), the balance favoring the former. As observed elsewhere, the difference here can be explained in terms of the structural role of radical SOMO (singly occupied molecular orbital), which is both E–E and E–N antibonding.[3] In the cation this orbital is empty, and its occupation, in the radical or its dimer, leads to lengthening of the E–N and, more particularly, the E–E bonds.[16] Insofar as the effect of the two electrons present in 4 is spread over three rings, the

(12) Hazell, A.; Hazell, R. G. *Acta Crystallogr.* **1988**, *C44*, 1807.
(13) Scholz, U.; Roesky, H. W.; Schimkowiak, J.; Noltemeyer, M. *Chem. Ber.* **1989**, *122*, 1067.
(14) Del Bel Belluz, P.; Cordes, A. W.; Kristof, E. M.; Kristof, P. V.; Liblong, S. W.; Oakley, R. T. *J. Am. Chem. Soc.* **1989**, *111*, 9276.
(15) Vegas, A.; Pérez-Salazar, A.; Banister, A. J.; Hey, R. G. *J. Chem. Soc., Dalton Trans.* **1980**, 1812.

Table 4. Summary of Intermolecular E- - -E and E- - -N Contacts (angstroms) in 4 (E = S, Se).[a] ESDs in Parentheses

E = S	
S1–S21 (at $-x, 1-y, 2-z$)	3.961(5)
S1–S11 (at $-x, 1-y, 2-z$)	4.084(5)
S11–S11 (at $-x, 1-y, 2-z$)	3.947(7)
S2–S22 (at $1-x, 1-y, 2-z$)	4.103(5)
S2–S12 (at $1-x, 1-y, 2-z$)	4.114(5)
S12–S12 (at $1-x, 1-y, 2-z$)	3.980(6)
E = Se	
Se21–Se1 (at $1-x, 2-y, 1-z$)	4.008(12)
Se21–Se11 (at $1-x, 2-y, 1-z$)	4.094(13)
Se11–Se11 (at $1-x, 2-y, 1-z$)	3.995(17)
Se2–Se22 (at $1-x, 1-y, 1-z$)	3.973(13)
Se2–Se12 (at $1-x, 1-y, 1-z$)	4.092(15)
Se12–Se12 (at $1-x, 1-y, 1-z$)	3.993(20)
Se1–Se22 (at $1+x, y, z$)	4.005(15)
Se1–N2 (at $2-x, 1-y, 1-z$)	3.64(5)
Se2–N1 (at $2-x, 1-y, 1-z$)	3.65(5)
Se21–N22 (at $-x, 2-y, 1-z$)	3.67(5)
Se22–N21 (at $-x, 2-y, 1-z$)	3.58(5)

[a] The coordinates refer to the symmetry position of the second atom.

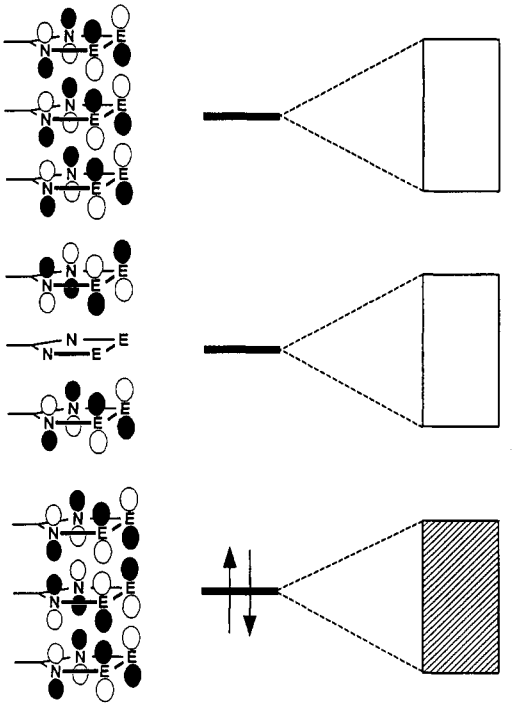

Figure 2. Qualitative energy level diagram for the frontier orbitals of the trimeric $[PhCN_2E_2]_3^+$ cation (E = S, Se), and the resulting solid-state band structure.

lengthening is not expected to be as great as in the simple dimers **3**. Figure 2 illustrates a qualitative MO diagram for the interaction of the SOMOs of three CN_2E_2 rings. Given the formal positive charge on **4**, the occupation level and phase pattern is reminiscent of those seen in the π-manifold of the allyl cation; only the lowest orbital, which is bonding with respect to the interannular interactions, is occupied. Interannular binding within the trimer units is therefore weak; the entire trimer unit is essentially held together by just two electrons. The mean E- - -E contacts (3.181/3.377 Å for E = S/Se) are thus predictably longer

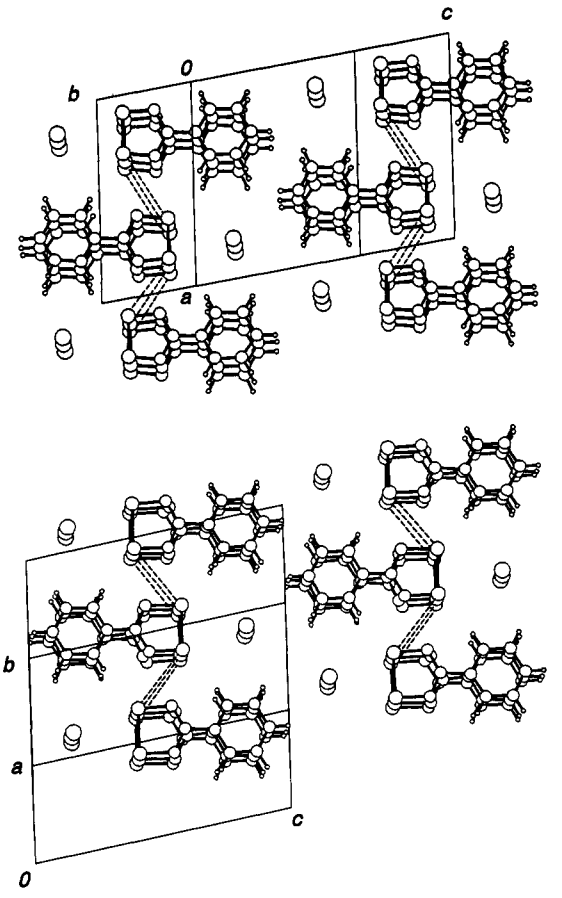

Figure 3. Packing patterns of $[PhCN_2E_2]_3[I_3]$, E = S (above) and Se (below), showing lateral E- - -E contacts (dashed lines).

than the interdimer E- - -E distances seen in **4** (R = Ph, 3.109/3.254 Å for E = S/Se).

Figures 3–5 provide comparative views of the packing patterns for the two structures. When viewed from a direction approximately perpendicular to the plane of the heterocyclic rings (Figure 3) the crystal structures appear remarkably similar. In both cases the molecular units form ribbons which run to-and-fro in antiparallel arrays; within each ribbon a triiodide iodine follows onto the tail of the next phenyl ring. The associatied dovetailing of heterocyclic rings gives rise to a series of lateral E- - -E contacts (see also Figure 4 and Table 4). Given the van der Waals radii[17] of S (1.80 Å) and Se (1.90 Å), and in comparison to similar contacts seen in the structures of neutral dimers, these contacts are relatively long. In contrast to the perspective shown in Figure 3, the arrangements of the ribbons of trimers as viewed from the side are quite different (Figure 5). For the sulfur compounds consecutive layers of molecular ribbons run in the same direction. Moreover, the layers are offset, so that each heterocyclic trimer is sandwiched between and a triiodide and set of phenyl rings, i.e., there is no opportunity for extended interactions perpendicular to the layered ribbons. By contrast, in the selenium compound, consecutive layers run antiparallel, with a dovetailed overlap between each timer unit and those above and below. While the intertrimer Se- - -Se contacts (4.233 and 4.497 Å) occasioned by this dovetailed overlap are relatively remote, the Se- - -N interactions (Table 4) are close to the van der Waals separation for Se (radius 1.90 Å) and N (radius 1.55

(16) Cordes, A. W.; Bryan, C. D.; Davis, W. M.; DeLaat, R. H.; Glarum, S. H.; Goddard, J. D.; Haddon, R. C.; Hicks, R. G.; Kennepohl, D. K.; Oakley, R. T.; Scott, S. R.; Westwood, N. P. C. *J. Am. Chem. Soc.* **1993**, *115*, 7232.

(17) Bondi, A. *J. Phys. Chem.* **1964**, *68*, 441.

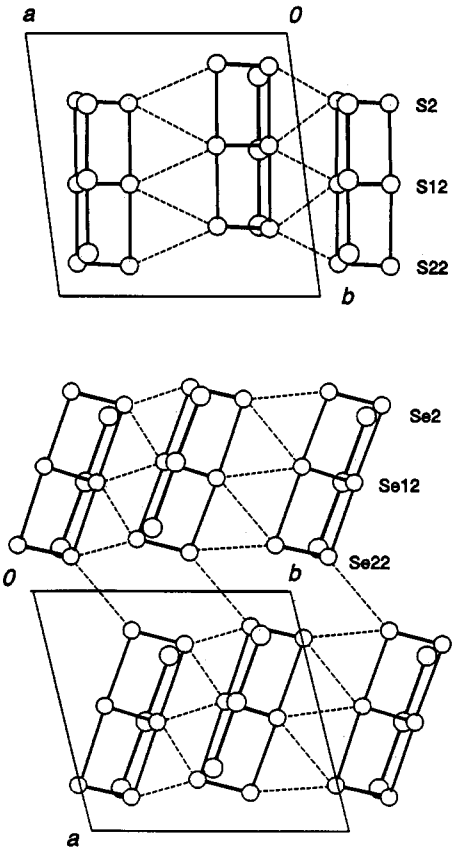

Figure 4. End-on view of sets of $[E_2]_3[I_3]$ units, showing lateral E- - -E contacts (dashed lines).

Å)[17] and may well provide a mechanism for electronic communication along the dovetailed stacks of trimers.

Crystals of $[PhCN_2S_2][I_3]$ belong to the monoclinic space group $P2_1/a$. An ORTEP drawing of a single cation/anion pair is provided in Figure 6; atomic (non-hydrogen) coordinates are shown in Table 5 and a summary of intramolecular distances is provided in Table 6. The molecular structure is comprised of a single heterocyclic cation and an associated triiodide anion. The internal structure features of the CN_2S_2 ring are similar to those found in other simple salts and are consistent with a full positive charge on the heterocycle (*vide supra*). The triiodide weakly coordinates to the ring through two long (3.562 and 3.352 Å) S- - -I contacts to a single terminal iodine atom (I1).

Figure 7 illustrates the packing pattern for $[PhCN_2S_2][I_3]$. In contrast to both the neutral materials and the mixed valence compounds described here, and consistent with other $PhCN_2S_2^+$ salts, the heterocyclic units are well separated (there is no stacking). The packing of the planar cations and anions results in two-dimensional "sheets" in the *yz* plane. Within the plane there are rows of $PhCN_2S_2^+$ cations alternating with rows of triiodide anions.

Band Structure Calculations. To probe the electronic consequences of the structural differences noted above we have performed a series of extended Hückel band structure calculations on the mixed valence compounds. Here, as elsewhere,[18,19] we have elected to focus the calculation by replacing the phenyl groups by hydrogen

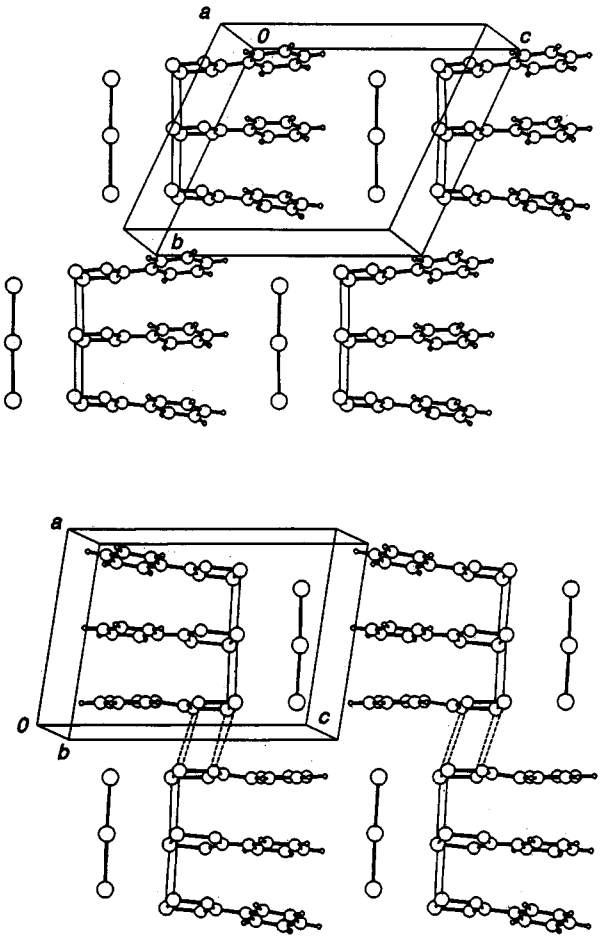

Figure 5. Layers of $[PhCN_2E_2]_3[I_3]$ ribbons, E = S (above) and Se (below), showing intertrimer Se- - -N contacts (dashed lines).

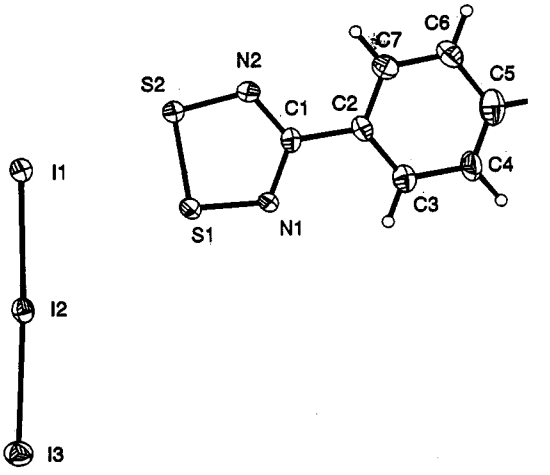

Figure 6. ORTEP drawing (30% ellipsoids) of $[PhCN_2S_2][I_3]$.

atoms; the triiodides have also been omitted. These simplifications have no effect on the valence and conduction bands, which are exclusively based on the heterocycle. The results, expressed as density of states (DOS) diagrams (Figure 8), can be understood with reference to the simplified band scheme developed above; the three flagged bands thus correspond to those developed from the three molecular orbital combinations illustrated in Figure 2. In the sulfur compound, in which stacking of trimers is absent, only lateral interactions serve to broaden the three bands, and the calculated bandgap is 0.8 eV. In the selenium compound, in which dovetailed stacking is

(18) Cordes, A. W.; Haddon, R. C.; Hicks, R. G.; Kennepohl, D. K.; Oakley, R. T.; Palstra, T. T. M.; Schneemeyer, L. F.; Scott, S. R.; Waszczak, J. V. *Chem. Mater.* **1993**, *5*, 820.

(19) Davis, W. M.; Hicks, R. G.; Oakley, R. T.; Zhao, B.; Taylor, N. *Can. J. Chem.* **1993**, *71*, 180.

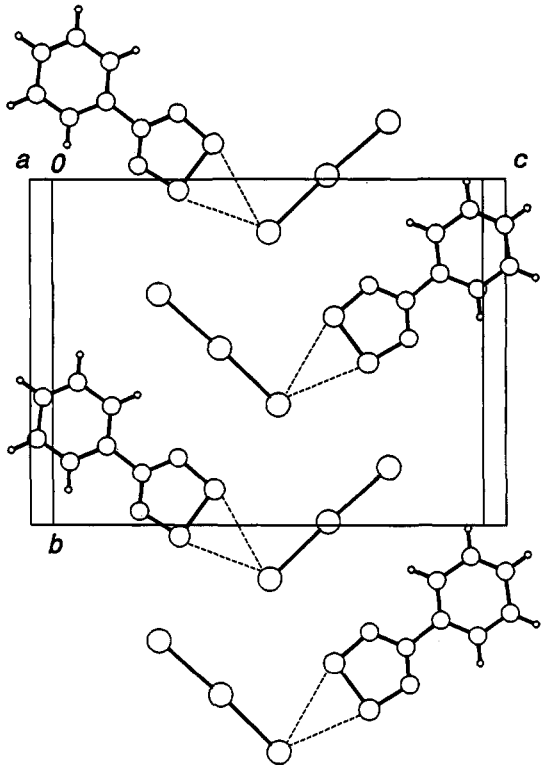

Figure 7. Projection of a single layer of $[PhCN_2S_2][I_3]$, showing S- - -I contacts (dashed lines).

Table 5. Non-Hydrogen Atomic Parameters *x*, *y*, *z*, and B_{eq} for $[PhCN_2S_2][I_3]$. ESDs Refer to the Last Digit Printed

	x	*y*	*z*	B_{eq}[a]
I1	0.82205(7)	0.34687(4)	0.49395(3)	3.423(24)
I2	0.69203(6)	0.51099(4)	0.61666(3)	3.053(21)
I3	0.56677(8)	0.66725(4)	0.74570(4)	4.13(3)
S1	0.7697(3)	0.60347(15)	0.36838(12)	3.22(8)
S2	0.8402(3)	0.46897(15)	0.29525(13)	3.43(8)
N1	0.7711(9)	0.6941(5)	0.2900(4)	3.4(3)
N2	0.8548(8)	0.5407(5)	0.2070(4)	3.13(25)
C1	0.8199(9)	0.6501(5)	0.2121(5)	2.9(3)
C2	0.8284(10)	0.7275(6)	0.1353(5)	3.1(3)
C3	0.8130(11)	0.8421(6)	0.1441(6)	3.7(3)
C4	0.8235(14)	0.9109(7)	0.0698(6)	4.8(4)
C5	0.8488(13)	0.8677(9)	−0.0050(7)	5.1(5)
C6	0.8687(12)	0.7477(8)	−0.0159(5)	4.2(4)
C7	0.8611(12)	0.6818(6)	0.0559(6)	3.9(4)

[a] B_{eq} is the mean of the principal axes of the thermal ellipsoid.

Table 6. Mean Intramolecular Distances (angstroms) and Angles (deg) in $[PhCN_2S_2][I_3]$. ESDs in Parentheses

S–S	2.027(3)	I1–I2	2.9081(8)
N–S	1.595(5)	I2–I3	2.9010(8)
N–C	1.342(10)		
S–S–N	95.2(2)	I1–I2–I3	177.34(2)
S–N–C	115.1(5)		

observed, the three bands are noticeably broadened, and the bandgap consequently reduced to 0.4 eV.

The dispersion curves for the highest occupied (in- and out-of-phase) and lowest unoccupied (in- and out-of-phase) crystal orbitals, as plotted along the principal axes of reciprocal space (Figure 9), afford a more detailed insight into the extent and dimensionality of interannular interactions. In the sulfur compound dispersion is minimal in all three directions, as expected. Indeed dispersion of any degree is only apparent along *X*, this direction being approximately equivalent (in real space) to lateral interactions in the *x* direction (real space). In the selenium compound, the correspondence between real and reciprocal unit cell vectors is closer, since all the unit cell angles are near 90°. Dispersion along *Z* is again negligible, as expected given the absence of interannular contacts in the *z* direction (real space). The strong dispersion along *X*, coupled with the smaller but still significant dispersion along *Y*, reflects the rather two-dimensional nature of the electronic structure.

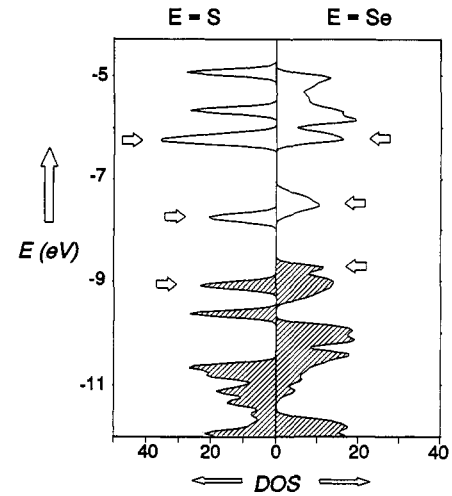

Figure 8. Calculated density of states (states/eV cell) for model $[HCN_2E_2]_3^+$ lattices based on $[PhCN_2E_2]_3[I_3]$ (E = S, Se) structures. Bands indicated with arrows arise from the three MO combinations shown in Figure 2.

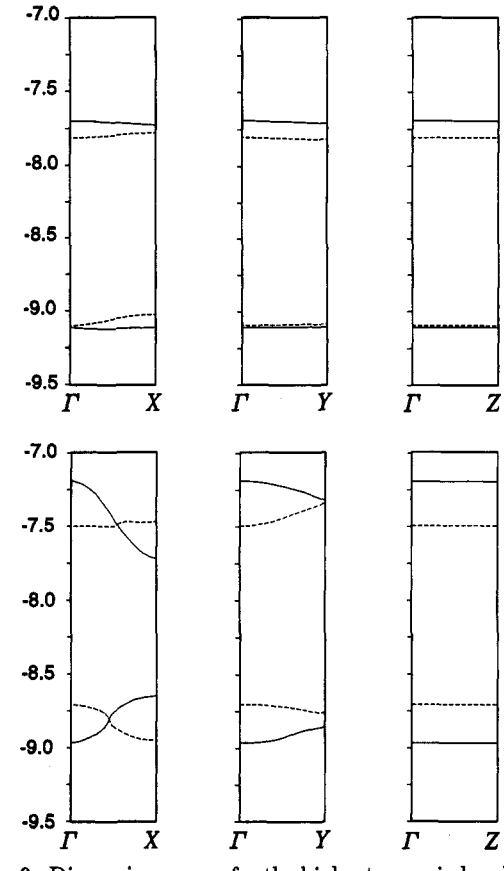

Figure 9. Dispersion curves for the highest occupied and lowest unoccupied crystal orbitals for model $[HCN_2E_2]_3^+$ lattices based on $[PhCN_2E_2]_3[I_3]$ (E = S, Se) structures. The solid lines represent the in-plane combinations of molecular orbitals; the dashed lines represent the out-of-phase combinations.

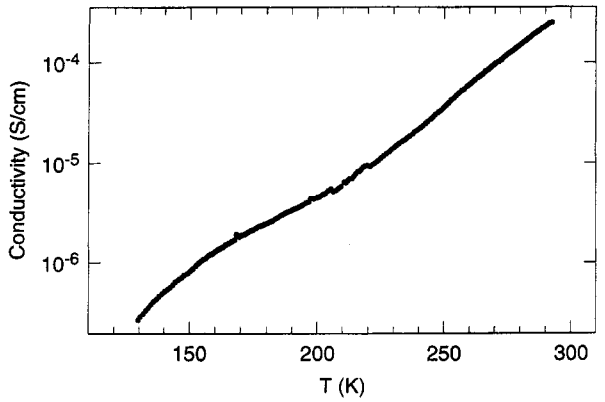

Figure 10. Variable temperature single crystal conductivity of 4 (E = Se).

Conductivity and Magnetic Measurements. Preliminary pressed pellet conductivity measurements on $[PhCN_2E_2]_3[I_3]$ (E = S, Se) confirmed, as expected, a relatively weak room-temperature conductivity (near 10^{-6} S cm^{-1}) for the sulfur compound. The selenium derivative showed more promise, and its transport properties were therefore investigated more fully. Single crystals of $[PhCN_2Se_2]_3[I_3]$ were wired for four-point conductivity measurements along the needle axis; wires were attached with gold paint. The single-crystal conductivity of the material, as measured over the temperature range 130–300 K is shown in Figure 10. The conductivity is activated, rising to a value of 10^{-4} S cm^{-1} at room temperature. Analysis of the high-temperature data affords an activation energy of 0.29 eV. The magnetic susceptibility of $[PhCN_2Se_2]_3[I_3]$ was measured between 2 K and room temperature using a Quantum Design SQUID magnetometer at 1 T. The signal was diamagnetic throughout the measurement, and the diamagnetism was found to be 140×10^{-6} emu mol^{-1}, in good agreement with Pascal's constants. The susceptibility showed a small Curie tail, arising from a residual spin concentration of <1% on a per molecule basis.

Summary and Conclusions

In previous papers we have described the solid state structural and transport properties of neutral dimers of the type $[1]_2$. These materials (for E = Se) are semiconductors, with a suggested conduction mechanism which involves thermal activation of electrons across a bandgap. The size of this bandgap can be closely correlated with structure, such that more densely packed structures, with more widely dispersed valence and conduction bands, have smaller experimental and predicted (by band calculation) bandgaps. The molecular unit 4 described here represents a novel extension of the neutral dimer approach to molecular conductors. As a natural consequence of the two-electron three-center (2e–3c) orbital manifold which binds this molecular unit together, the separation of the valence and conduction bands is reduced (by a factor of $1\sqrt{2}$ at the Hückel level), regardless of the extent of intermolecular interactions. In the case of $[PhCN_2Se_2]_3[I_3]$, the crystal packing affords intermolecular contacts which are relatively small in comparison to those seen in some neutral dimers, i.e., the packing is not particularly efficient. However, when coupled with the initially smaller band spreading associated with the intramolecular 2e–3c binding, the dispersive effect of the intermolecular interactions leads to a solid-state structure for which the predicted (EHMO) and measured bandgap is remarkably small.

As with the neutral dimers, chemical modification of the exocyclic R group in 4 may afford materials with more efficient crystal packing (tighter intermolecular E- -E contacts) and even better conductivity characteristics. We are therefore investigating the structures and transport properties of other CT salts of simple monofunctional radicals. In contrast to early observations,[7] these materials exhibit good thermal stability, and a rich chemistry in terms of stoichiometric ratio (radical:iodine) is anticipated.

Experimental Section

Starting Materials and General Procedures. Iodine, KI, and *n*-Bu_4NI were obtained commercially (Fisher) and used as received. Acetonitrile (Fisher HPLC grade) was purified by distillation from P_2O_5. The 4-phenyl-1,2,3,5-dithia- and diselenadiazolyl radicals and the PF_6^- salts of the corresponding cations were prepared according to literature methods.[6,14] All reactions (in solution) were performed under vacuum or under an atmosphere of nitrogen. The gas-phase reactions were performed in ATS series 3210 three-zone tube furnace, linked to a Series 1400 temperature control system. Infrared spectra were recorded on a Nicolet 20SX/C FTIR spectrometer. Elemental analyses were performed by MHW Laboratories, Phoenix, AZ. Melting-point determinations were made on samples in tubes sealed under argon.

Preparation of $[C_6H_5CN_2E_2]_3[I_3]$ (E = S, Se) in the Gas Phase. In a typical experiment, iodine (0.252 g, 1.0 mmol) and 1 mol equiv of $[PhCN_2E_2]_2$ were sealed in an evacuated (10^{-3} Torr) Pyrex tube (25 mm × 250 mm). That half of the tube containing both reagents was slowly ramped over a period of several days from 50 to 80 °C (for sulfur) and 70 to 120 °C (for selenium). Throughout this period the other half of the tube was maintained at 55 °C (for sulfur) and 60 °C (for selenium). Over the course of 5 weeks (for sulfur) and 2 weeks (for selenium), deep blue needles grew in the cooler portion of the tube. These mildly air-sensitive crystals were harvested in a drybox and stored under a nitrogen or argon atmosphere. Yields were as high as 80%, although values of 40–50% were more typical. E = S: Ir (2000–200 region, Nujol mull, CsI optics) 1597 (w), 1459 (vs), 1376 (vs), 1261 (w), 1171 (w), 1130 (m), 1023 (m), 901 (m), 859 (w), 823 (w), 787 (s), 722 (m), 689 (m), 517 (s), 456 (s) cm^{-1}. MP 160–165 °C (dec). Anal. Calcd for $C_7H_5IN_2S_2$: C, 27.28; H, 1.64; N, 9.0; I, 41.18%. Found: C, 27.38; H, 1.77; N, 9.02; I, 41.00%. E = Se: IR (2000–200 cm^{-1}) 1463 (vs), 1451 (s), 1377 (s), 1312 (m), 1258 (w), 1221 (vw), 1154 (w), 1115 (m), 1022 (m), 737 (m), 723 (m), 704 (vs), 688 (s), 666 (m), 611 (s), 424 (s), 290 (m) cm^{-1}. MP 207–212 °C (dec). Anal. Calcd for $C_7H_5IN_2Se_2$: C, 20.92; H, 1.25; N, 6.97; I, 31.57%. Found: C, 21.12; H, 1.36; N, 6.96; I, 32.03%.

Preparation of $[C_6H_5CN_2S_2]_3I_3$ in Acetonitrile. (a) From $[C_6H_5CN_2S_2]_2$ and Iodine. A solution of iodine (200 mg, 1.58 mmol) in 15 mL of acetonitrile was added to a solution of $[C_6H_5CN_2S_2]_2$ (285 mg, 1.57 mmol) in 35 mL of acetonitrile. A greenish-brown solid immediately precipitated. The solid dissolved on heating, giving a deep wine-red solution. Slow cooling of the solution produced very fine blue-metallic needles. The needles were filtered, rinsed with 2 × 10 mL of cold acetonitrile, and dried *in vacuo* (yield 370 mg, 76%). The infrared spectrum of this material was identical to that of the product of the gas-phase reaction described above.

(b) From $C_6H_5CN_2S_2^+Cl^-$ and KI. Acetonitrile (50 mL was syringed into a sidearm flask containing 4-phenyl-1,2,3,5-dithiadiazolium chloride (410 mg, 1.9 mmol) and finely ground potassium iodide (330 mg, 2.0 mmol). The slurry quickly darkened, and a greenish-brown precipitate formed. The mixture was refluxed for 30 min and hot filtered to remove the KCl precipitate. The wine-red filtrate was slowly cooled to give metallic blue needles, which were then filtered, rinsed with 2 × 10 mL of cold acetonitrile, and dried *in vacuo* (yield 360 mg, 61%). The infrared spectrum of this material was identical to

that of $[C_6H_5CN_2S_2]_3I_3$ prepared by the other two routes as described above.

Preparation of $[C_6H_5CN_2Se_2]_3I_3$ in Acetonitrile. A solution of tetra-*n*-butylammonium iodide (240 mg, 0.65 mmol) in 10 mL of CH_3CN was added dropwise to a solution of $C_6H_5CN_2Se_2^+PF_6^-$ (275 mg, 0.65 mmol) in 20 mL of CH_3CN. A black solid was produced immediately. The mixture was stirred for 30 min at room temperature and filtered. The black solid was rinsed with 3 × 10 mL of CH_3CN and pumped to dryness to give crude $[C_6H_5CN_2Se_2]_3I_3$ (yield 210 mg, 80%). The crude material was sublimed under static vacuum (*ca.* 100 °C/10^{-2} Torr) in a sealed tube to give thin blue needles, yield 175 mg (76%). The infrared spectrum of this material was identical to that of the product of the gas-phase reaction described above.

Preparation of $C_6H_5CN_2S_2I_3$. In a typical experiment, iodine (510 mg, 4.04 mmol) and $[C_6H_5CN_2S_2]_2$ (220 mg, 1.21 mmol) were sealed in an evacuated (10^{-3} Torr) Pyrex tube. The end of the tube containing both reagents were heated initially to 70 °C and then slowly raised over a 3-week period to 90 °C, while the far end of the tube was similarly ramped from 45 to 60 °C. Lustrous dark copper rodlike crystals slowly formed at the far end. The mildly air-sensitive crystals were harvested and stored under an inert atmosphere (nitrogen or argon). The residue still appeared to contain significant amounts of material; however, leaving the sublimation for longer periods of time in attempts to increase yields invariably resulted in thermal decomposition of the crystals to $[C_6H_5CN_2S_2]_3I_3$ and iodine. Raising the sublimation temperature beyond 90 °C to try and shorten the sublimation period also led to decomposition to $[C_6H_5CN_2S_2]_3I_3$. Yields were *ca.* 35%. IR (2000–200-cm^{-1} region) 1463 (s), 1377 (s), 1146 (m), 1023 (m), 921 (w), 891 (m), 828 (s), 803 (w), 771 (m), 722 (w), 684 (s), 663 (w), 540 (s), 366 (m), cm^{-1}. Anal. Calcd for $C_7H_5N_2S_2I_3$: C, 14.96; H, 0.90; N, 4.98; I, 67.75%. Found: C, 15.20; H, 0.87; N, 4.97; I, 68.00%.

X-ray Measurements. All X-ray data were collected on an ENRAF-Nonius CAD-4 diffractometer with monochromated Mo Kα (λ = 0.710 73 Å) radiation. Crystals were mounted on a glass fiber with epoxy. Data were collected using a $\theta/2\theta$ technique. The structures were solved using direct methods/SOLVER and refined by full-matrix least-squares analysis which minimized $\sum w(\Delta F)^2$. A summary of crystallographic data is provided in Table 7. As with other systems of this type, crystals of the selenium compound readily twin; the data set used for this report is one of three complete data sets collected; at least 13 different crystals were actually mounted on the diffractometer in order to find those with minimal twinning. The extent twinning of the data crystals was observed on Weissenberg photographs. However, attempts to unravel the twinning were unsuccessful. In the refinement reported here the benzene ring was modeled by an idealed carbon skeleton with hexagonal symmetry (C–C = 1.39 Å). Each moiety was refined with group anisotropic displacement parameters. The temperature (factors of all six selenium atoms in the asymmetric unit were refined as a single set of anisotropic displacement parameters, although the positional refinement was individualized. The N–C–N moiety was refined as a unit with isotropic temperature factors and a constrained geometry with N–C = 1.34 Å and N–C–N = 125 °C. These average values resulted from unconstrained refinement utilizing SHELXL-93 and all measured reflections.

Table 7. Crystal Data for 4 (E = S, Se) and $[PhCN_2S_2][I_3]$

formula	$IS_2N_2C_7H_5$	$ISe_2N_2C_7H_5$	$I_3S_2N_2C_7H_5$
fw	308.15	401.95	561.96
a, Å	10.278(4)	10.368(6)	7.366(4)
b, Å	11.508(2)	10.818(8)	11.734(1)
c, Å	13.333(4)	13.421(8)	15.166(2)
α, deg	114.97(2)	80.64(5)	
β, deg	99.21(3)	81.20(5)	95.92(?)
γ, deg	92.65(2)	75.18(6)	
V, Å^3	1399.7(7)	1426(2)	1303.9(7)
d(calcd), g cm^{-3}	2.19	2.81	2.86
space group	$P\bar{1}$	$P\bar{1}$	$P2_1/a$
μ, mm^{-1}	3.77	10.86	7.40
λ, Å	0.710 73	0.710 73	0.710 73
temp, K	293	293	293
$R(F^2)$, R_w $(F^2)^a$	0.045, 0.063	0.093, 0.114[b]	0.029, 0.056

[a] $R = [\sum||F_o| - |F_c||]/[\sum|F_o|]$; $R_w = \{[\sum w||F_o| - |F_c||^2]/[\sum(w|F_o|^2)]\}^{1/2}$. [b] High *R* values are the result of unresolved twinning problems (see text).

Band Structure Calculations. The band structure calculations were carried out with the EHMACC suite of programs using the parameters discussed previously.[6,20] The phenyl groups were replaced by a hydrogen atom at the site of the ipso carbon, and the iodines were not included. The off-diagonal elements of the Hamiltonian matrix were calculated with the standard weighting formula.[21]

Acknowledgment. Financial support at Guelph was provided by the Natural Sciences and Engineering Research Council of Canada (NSERC) and at Arkansas by the National Science Foundation (EPSCOR program). C.D.B. acknowledges a DOE/ASTA Traineeship.

Supplementary Material Available: Tables of crystal data, structure solution and refinement, atomic coordinates, bond lengths and angles, anisotropic thermal parameters for $[PhCN_2E_2][I_3]$ (E = S, Se) and $[PhCN_2S_2][I_3]$ (10 pages); observed and calculated structure factors (42 pages). Ordering information is given on any current masthead page.

(20) Basch, H.; Viste, A.; Gray, H. B. *Theor. Chim. Acta* **1965**, *3*, 458.
(21) Ammeter, J. H.; Burghi, H. B.; Thibeault, J. C.; Hoffmann, R. *J. Am. Chem. Soc.* **1978**, *100*, 3686.